

# 2D line-scan photoacoustic imaging of absorbers in a scattering tissue phantom

Beard PC<sup>1</sup> and Mills TN

Department of Medical Physics and Bioengineering, University College London, Shropshire House,  
11-20 Capper Street, London WC1E 6JA, UK

## ABSTRACT

A photoacoustic imaging system has been evaluated by mapping the temporal distribution of photoacoustic signals generated in a tissue phantom. The phantom comprised an Intralipid scattering solution ( $\mu_s'=1\text{mm}^{-1}$  and  $\mu_a=0.01\text{mm}^{-1}$ ) containing two regions of enhanced absorption; a 1.5mm thick layer ( $\mu_a=1\text{mm}^{-1}$ ) and a 75 $\mu\text{m}$  layer ( $\mu_a=40\text{mm}^{-1}$ ). These were located 1cm beneath the surface of the Intralipid which was irradiated with 7ns Q switched laser pulses of fluence 0.05 J/cm<sup>2</sup>. A Fabry Perot polymer film ultrasound sensing interferometer was used for the detection of the photoacoustic signals. A 1D ultrasound array was simulated by illuminating the sensing interferometer with a large diameter laser beam and line scanning a photodiode across the reflected output beam. The detection sensitivity of the system was 3kPa over a 25MHz measurement bandwidth, the 3dB acoustic bandwidth was 17.5MHz, the sensitive azimuthal "array" aperture and element size were 12mm and 0.8mm respectively. Greyscale images of the time-resolved photoacoustic signals enabled both absorbers to be clearly identified with an axial spatial resolution of less than 100 $\mu\text{m}$ . It is envisaged that this approach could form the basis of a practical photoacoustic tissue imaging system.

*Keywords: Photoacoustic, thermoacoustic, imaging, ultrasound array, biomedical, Fabry Perot sensor.*

## 1. INTRODUCTION

Photoacoustic or thermoacoustic imaging is a soft tissue imaging modality in which sub-microsecond pulses of optical or microwave electromagnetic radiation are used to excite subsurface acoustic waves on to which the spatial and functional properties of the tissue are encoded. The signal generation process is one in which the absorption of the incident pulsed radiation leads to impulsive heating of the irradiated tissue volume followed by rapid thermoelastic expansion and the subsequent generation of broadband ultrasonic thermoelastic waves. These propagate to the surface where they are detected by an array of ultrasound transducers. The detected signals can then be spatially resolved and back-projected in 3 dimensions to re-construct a volumetric image of the internally absorbed electromagnetic energy distribution from which a 3D representation of the internal tissue structure can be extracted. The penetration depths that can be achieved depend upon the attenuation of the excitation radiation in the tissue and the signal losses due to frequency dependent attenuation of ultrasound in tissue with the latter also determining axial spatial resolution. Depths of several cm with mm spatial resolution using both microwave<sup>1</sup> and NIR (near-infrared) laser excitation<sup>2</sup> have been reported for applications such as breast imaging for the detection of cancerous lesions. Higher spatial resolution (<100 $\mu\text{m}$ ) has been demonstrated with sub-cm penetration depths for applications such as imaging skin and superficial blood vessels<sup>3</sup>.

---

<sup>1</sup> Correspondence to P. Beard, Dept of Medical Physics, UCL, Shropshire House, 11-20 Capper Street, London WC1E 6JA, UK, email: [pbeard@medphys.ucl.ac.uk](mailto:pbeard@medphys.ucl.ac.uk), <http://www.medphys.ucl.ac.uk/research/mle/research.htm>

The potential for high contrast is possibly the most widely proffered advantage of the technique. This is particularly so when optical excitation is used as it enables the large variation in the optical absorption and scattering properties of different tissue constituents to be exploited. Sources of naturally occurring absorption contrast include chromophores such as haemoglobin (and its various oxygenated states), melanin, beta-carotene, lipids whilst scattering based contrast arises from the presence of fibrous tissue, collagen, increased cellularity, and calcification. Of all of these, haemoglobin is perhaps the most significant. It offers strong optical contrast at visible and NIR optical wavelengths making the technique well suited to imaging blood vessels for directly assessing arterial disease or mapping the vasculature – by comparison, the contrast of conventional ultrasound images tends to be limited by the relatively poor echogenicity of blood vessels. It can also be exploited to indirectly detect abnormal tissue morphologies such as cancerous lesions and vascular lesions that are accompanied by changes in the surrounding vasculature and tissue oxygenation status.

A difficulty in implementing photoacoustic imaging techniques is associated with the detection of the photoacoustic signals. Ideally, for accurate image reconstruction the detectors should have a near-isotropic response at the maximum frequency component of the signal, an interelement spacing that fulfills the spatial Nyquist criterion ( $<\lambda/2$ ) and adequate detection sensitivity to detect the very weak acoustic signals generated at depth in the tissue. For high resolution applications where acoustic frequency components of several tens of MHz can be generated, this requires element sizes and interelement spacing of the order of 50 $\mu$ m and wideband detection sensitivities of approximately 1kPa. Such performance is difficult to achieve using piezoelectric transducer arrays. The complexity that arises from the need to incorporate a large number of electrical connections within the footprint of the array also presents difficulties. An additional difficulty is the requirement that, for many clinical applications, it is necessary to employ the so-called backward-mode of photoacoustic imaging where the acoustic signals are detected on the same side of the tissue that the excitation laser pulses are delivered to. Ideally, this requires a transparent sensor head through which the excitation pulses can be transmitted and generally precludes the use of a piezoelectric sensor head.

A solution to the detection problem may lie in optical methods whereby the incident acoustic field distribution, following an appropriate transduction process, is mapped on to an optical field. The spatial discretisation of the acoustic detection process can therefore be removed from the detection plane to a remotely located high-density array of optical detectors such as a photodiode array or CCD array. This offers intrinsic advantages in terms of the spatial sampling of the acoustic aperture. Specifically, substantially smaller element sizes (in principle down to the optical diffraction limit of a few  $\mu$ m) and interelement spacings than can be achieved with piezoelectric arrays are possible. Additionally, there is the prospect of fabricating a transparent sensor head for backward mode imaging.

Several approaches have been investigated. The detection of acoustically-induced changes in optical reflectance at a glass-liquid interface for 2D photoacoustic imaging<sup>4</sup> has been demonstrated. A system based upon frustrated total internal reflection due to acoustically induced displacement of silicon nitride membranes has been investigated for transmission ultrasound imaging.<sup>5</sup> Interferometric detection of acoustically-induced displacements across the surface of a pellicle<sup>6</sup> and the detection of changes in the optical thickness of a multilayer dielectric stack Fabry Perot (F-P) interferometer<sup>7</sup> and a glass etalon<sup>8</sup> have also been described for ultrasound imaging and field mapping.

The use of a polymer film Fabry Perot (FP) sensing interferometer as an ultrasound sensor has also been studied principally as a single point detector for various photoacoustic<sup>9</sup> and ultrasound measurement applications<sup>10,11,12</sup>. Recently we have extended the concept to a 2D ultrasound array and demonstrated its use for transmission ultrasound imaging and transducer field mapping applications<sup>13</sup>. Its potential as a detection system for photoacoustic imaging has also been proposed<sup>14</sup> and in this paper we report experimental results that confirm its suitability for this. Specifically, we show that it has sufficient sensitivity over a usefully large acoustic aperture (1cm) to localise regions of enhanced absorption in a realistic tissue phantom. An experimental arrangement in which a photodiode is mechanically line-scanned across the FP sensor head output to produce a 2D image of the temporal distribution of the incident acoustic field has been developed (section 2). Preliminary evaluation was performed by mapping a well defined and reproducible ultrasound field produced by a focussed ultrasound transducer (section 3.1). Thereafter a variety of tissue phantoms comprising a scattering liquid and various submerged absorbers were irradiated with nanosecond laser pulses and the resulting photoacoustic signals mapped to obtain a 2D image.

## 2. EXPERIMENTAL SET-UP

Figure 1 shows a schematic of the experimental set-up used. The sensor head comprises a polymer film FP interferometer fabricated by a 3 layer vacuum deposition process<sup>10</sup>. Firstly, a partially reflective aluminium coating was deposited on to a glass backing stub. This was followed by the vacuum deposition of a 40 $\mu\text{m}$  thick polymer layer (Parylene) followed by a second fully opaque aluminium coating. The two aluminium coatings provide the mirrors of the FP cavity. A wedge was formed on the optical input side of the sensor head to eliminate parasitic interference between the light reflected from the FP polymer sensing film and that from the front face of the backing stub. The opacity of the aluminium coatings means that the sensor head is not transparent and therefore could not be used for backward mode photoacoustic imaging. This would require wavelength selective dielectric coatings that are transmissive to the excitation laser pulses as described in reference 14. However it does provide a convenient means of initially evaluating the concept using a forward mode detection configuration.

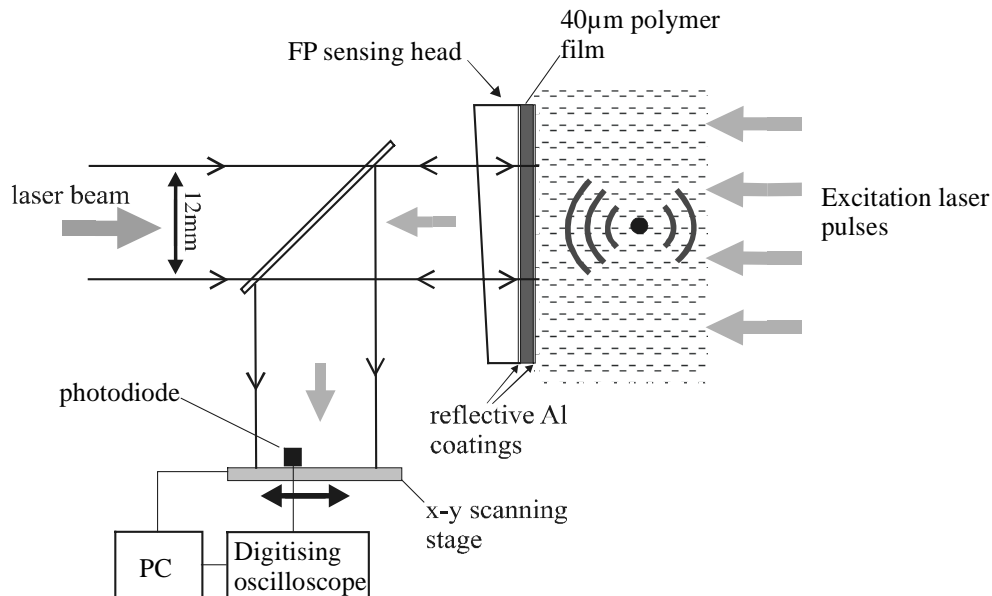


**Figure 1** Schematic showing experimental set-up for forward-mode photoacoustic imaging.

The FP sensor was interrogated with a collimated 15mW laser beam with a 12mm  $1/e^2$  beam diameter. The light reflected from the sensor was directed on to a 25MHz photodiode mounted on a PC controlled x-y scanning stage. The arrival of an acoustic wave from a photoacoustic source modulates the optical thickness of the polymer film producing a corresponding change in the intensity of the reflected beam. By scanning the photodiode across the reflected optical beam and capturing the time-varying photoacoustic signal at each point, the temporal and lateral distribution of the incident acoustic field can be mapped and subsequently backprojected to reconstruct an image of the target. To a first approximation (ie neglecting acoustic crosstalk) the effective element size and interelement spacing of the “array” can be taken to be those of the photodiode area (0.8mm diameter) and scan increment respectively.

The detection sensitivity was determined by referencing the sensor output to that of a calibrated PVDF membrane hydrophone giving a wideband (25MHz) noise-equivalent-pressure of 3kPa without signal averaging. The frequency response was not measured directly but a well-validated model<sup>11</sup> was used to predict its performance. As shown in figure 2, the sensor head design (40 $\mu$ m Parylene glass-backed configuration) employed in this study has a frequency response with a small  $\lambda/4$  resonance at 11MHz and a 3dB bandwidth of 17.5MHz. For comparison and to demonstrate the validity of the model, experimental and predicted frequency responses for two other sensor head configurations are also shown in figure 2.

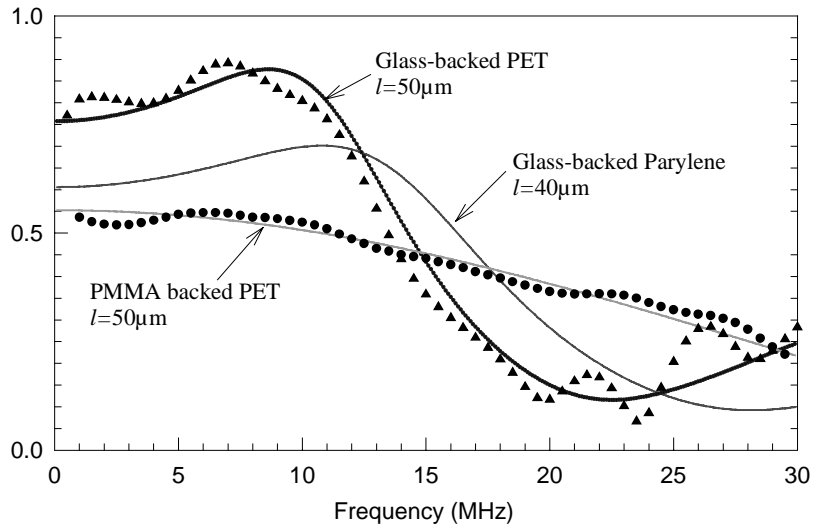


**Figure 2** Predicted (continuous lines) and measured (symbols) frequency responses of various backing configurations.

### 3. RESULTS

#### 3.1 PZT transducer field mapping

The experimental arrangement shown in figure 1 was initially evaluated using a well defined and stable ultrasound field provided by a pulsed 5MHz focussed piezoelectric PZT transducer. The photodiode was scanned along a line perpendicular to and passing through the axis of the transducer which was located above the sensor head in a water bath as shown in figure 3. At each point of the scan the acoustic waveform detected by the sensor was captured and linearly mapped to a greyscale to provide a visual representation of the temporal distribution of the incident acoustic field across the sensor head. Figure 3 shows this with the curvature of the wavefront clearly visible in the image over the 12mm line scan. The 2D lateral field distribution at various distances from the focus of this transducer has been previously reported in reference 13.

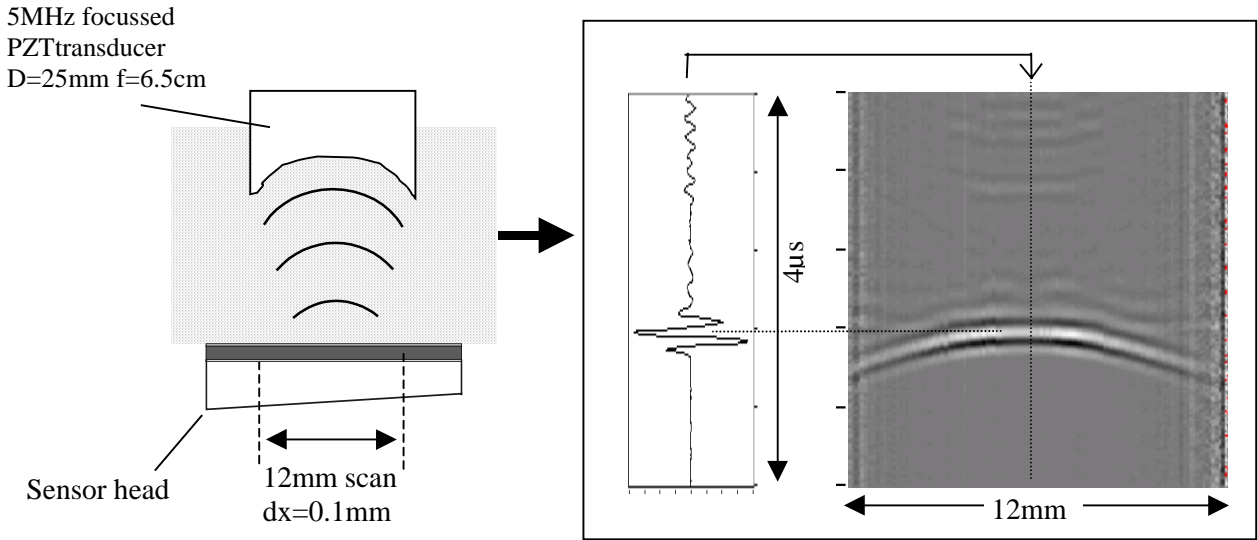


**Figure 3** Line scan through the axis of a pulsed focussed (PZT) 5MHz transducer. The waveform represents a profile through the centre of the image. A trigger delay (not shown) was used so the vertical axis begins at  $t=28\mu\text{s}$  – ie the sensor-transducer separation was approximately 4.5cm. Photodiode aperture: 0.8mm, transducer focal length: 6.5cm, transducer diameter: 25mm

## 3.2 Photoacoustic tissue phantom imaging

### 3.2.1 Depth profiling

To assess the penetration depth, axial spatial resolution and contrast that can be achieved, a tissue phantom comprising a scattering layer of an Intralipid solution of reduced scattering coefficient  $\mu_s=1\text{mm}^{-1}$  and absorption coefficient  $\mu_a=0.01\text{mm}^{-1}$  was used (figure 4). These optical properties were chosen to be approximately representative of tissues such as the breast,<sup>15</sup> skin<sup>16</sup> and muscle<sup>16</sup> in the near infrared (NIR). Two plastic sheets, one of thickness 1.5mm and  $\mu_a=1\text{mm}^{-1}$  and the other 75 $\mu\text{m}$  thickness and  $\mu_a=40\text{mm}^{-1}$  were submerged in the Intralipid. Both plastic sheets were approximately 1cm in width. The absorption coefficient of the 1.5mm thick absorber was chosen to provide an absorption contrast that might typically be provided by blood<sup>17</sup>. The purpose of the more strongly absorbing 75 $\mu\text{m}$  target was to provide a means of estimating axial spatial resolution rather than be representative of any particular tissue-optical properties. Nanosecond optical pulses from a frequency doubled Q switched Nd:YAG laser were passed through a negative lens to expand the beam to a diameter of 1cm and directed on to the surface of the phantom. This resulted in an incident surface fluence of  $0.02\text{J}/\text{cm}^2$  – well within the maximum permitted exposure (MPE) level for nanosecond pulsed laser irradiation in the NIR incident on skin<sup>18</sup>. The photoacoustic signals were detected by the sensor head at the bottom of the water bath – the so-called forward-mode of photoacoustic detection. The photodiode was scanned along a line across the sensor output beam. At each point of the scan, the detected time-dependent photoacoustic waveform was averaged over 100 shots and captured. The set of signals for the entire line scan were then linearly mapped to a greyscale and displayed as shown in figure 4. No further processing or image enhancement was performed.

Figure 4 shows that the signals from both plastic absorbers can be clearly identified. The thickness and depth profile of the 1.5mm absorber can be obtained by spatially resolving the time-varying signals (using the speed of sound in the absorber and the Intralipid respectively) at each point along the scan and then back projecting vertically along the line-of-sight at each detection position. The thickness and position of the 1.5mm absorber obtained from the image in this

way are in good agreement with the known values. Whilst this approach is valid for the 1.5mm absorber which lies parallel to the detection plane, care needs to be exercised in similarly identifying the position of the 75 $\mu$ m absorber. This is because it lies at an angle to the detection plane. The acoustic signal at each point along the scan therefore emanates not from a point vertically above it but one that is offset to the left. For such situations, where the photoacoustic source geometries are of large lateral extent and therefore emit near-planar waves, a far-field receive beamforming<sup>19</sup> approach would be required for accurate reconstruction of the image. When applied to tissue imaging however, where the lateral source dimensions are generally much smaller and the wavefronts non-planar, it is a near field<sup>3,20</sup> approach that is generally required.

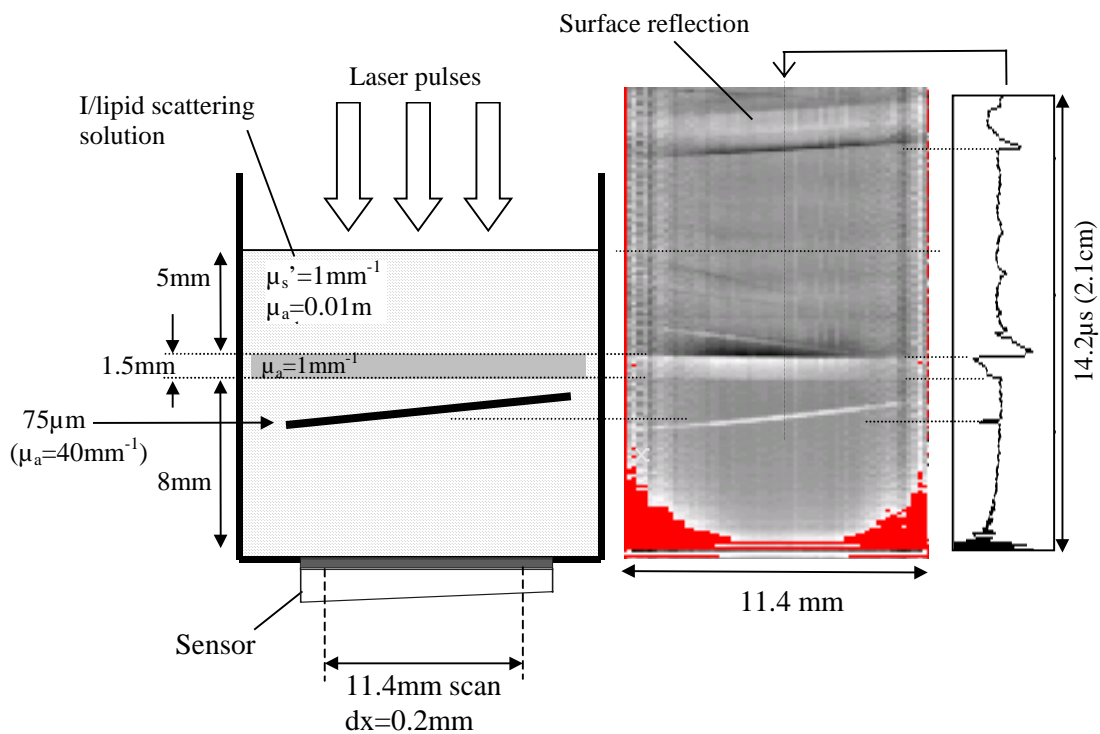


**Figure 4** Forward-mode photoacoustic depth profiling of plastic absorbers in a scattering liquid (Intralipid:  $\mu_s' = 1\text{mm}^{-1}$  and  $\mu_a = 0.01\text{mm}^{-1}$ ). The waveform on the far right represents a profile through the centre of the image. The “surface reflection” is the reflection of the photoacoustic signal generated in the 1.5mm absorber from the surface of the Intralipid. It appears at an angle because the water bath was slightly tilted. Incident laser fluence:  $0.02\text{ J/cm}^2$ , pulse duration:  $7\text{ns}$ .

Whilst the results in figure 4 clearly demonstrate the ability of this approach to localising regions of enhanced absorption in turbid media, a greater penetration depth than 5mm would be useful for biomedical tissue imaging. The above experiment was therefore repeated but with an increased Intralipid layer so that the 1.5mm absorber was now 10mm below the surface of the Intralipid. The beam diameter on the surface was reduced to 6mm thus increasing the fluence to  $0.05\text{J/cm}^2$  but still within the MPE. In all other respects the experimental procedure was identical. Figure 5 shows that the absorbers can still be clearly identified demonstrating that 1 cm penetration depth is feasible.

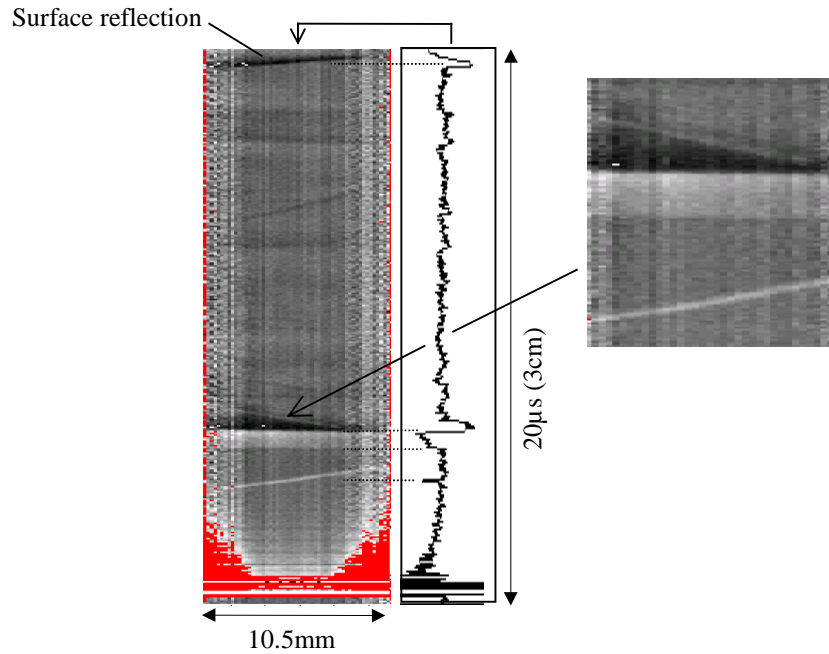


**Figure 5** Image shows results obtained using an identical arrangement to that depicted in figure 4 but with an increase from 5mm to 10mm in the thickness of the Intralipid layer ( $\mu_s=1\text{mm}^{-1}$  and  $\mu_a=0.01\text{mm}^{-1}$ ) above the 1.5mm plastic absorber ( $\mu_a=1\text{mm}^{-1}$ ). Incident laser fluence:  $0.05\text{ J/cm}^2$ , pulse duration:  $7\text{ ns}$ .

### 3.2.2 Localisation of a discrete absorber

The images shown in figures 4 and 5 were obtained using absorbing planar targets of large (1cm) lateral dimensions – ie comparable to the length of the line scan. In order to localise a discrete absorber, a 3mm wide strip of the 1.5mm thick plastic absorber ( $\mu_a=1\text{mm}^{-1}$ ) was placed perpendicular to and at the centre of the line to be scanned (figure 6). The absorber was situated at a depth of 10mm beneath the surface of the Intralipid scattering solution ( $\mu_s=1\text{mm}^{-1}$  and  $\mu_a=0.01\text{mm}^{-1}$ ) and 2.3mm above the sensor head. A line scan of length 10mm was performed and the resulting time-varying photoacoustic signals directly mapped to a linear grayscale as described in the preceding section. For this type of line-of-sight imaging the detector needs to be in the non-divergent near field of the photoacoustic source. From the lateral dimensions of the absorber (3mm) and estimating the acoustic wavelength at 1.5mm the absorber should be no further than 1.5mm away from the detector if it is to lie in the near field. This is not the case with the arrangement shown in figure 6 where the absorber-detector separation is 2.3mm. As a consequence the lateral boundaries of the absorber appear somewhat indistinct. The applicability of this type of line-of-sight imaging is limited by the lateral resolution constraints imposed by the source-detector separation requirements making synthetic receive focussing or radial backprojection methods more generally applicable to photoacoustic tissue imaging.

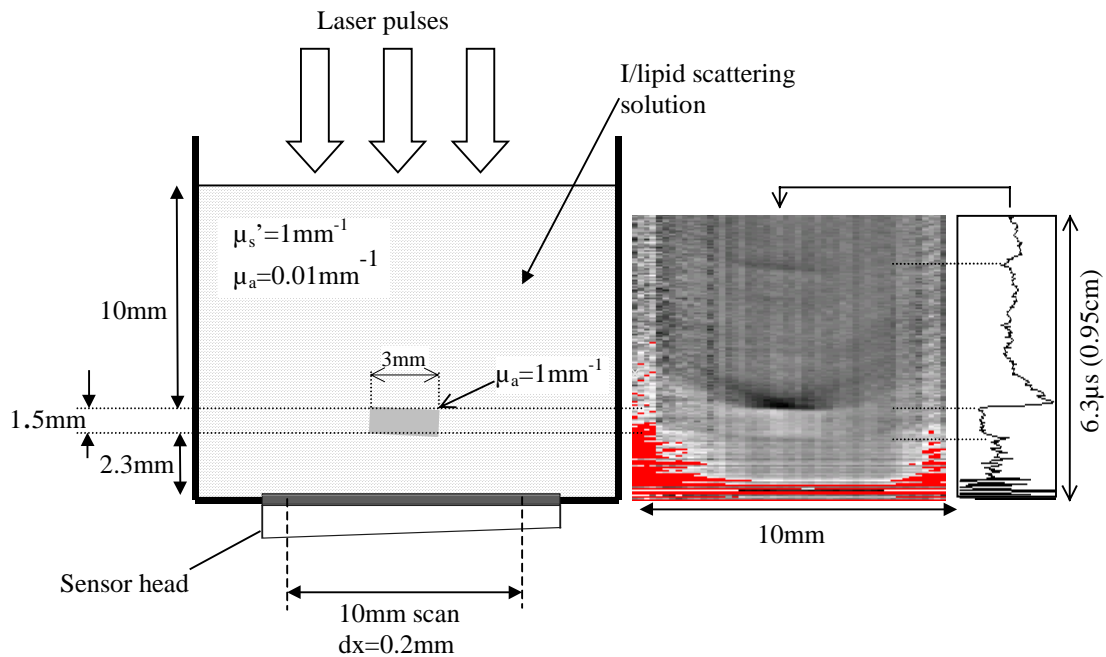


**Figure 6** Forward-mode photoacoustic localisation of a discrete absorber. The waveform on the far right represents a profile through the centre of the image. Incident laser fluence:  $0.05 \text{ J/cm}^2$ . Pulse duration:  $7 \text{ ns}$ .

#### 4. CONCLUSIONS

A forward mode photoacoustic imaging configuration employing a Fabry Perot polymer film sensing interferometer has been used to localise regions of enhanced absorption in a tissue phantom. This study suggests that the system would have sufficient sensitivity over a 1cm aperture to image a blood vessel at a depth of 1cm with an axial resolution of less than  $100 \mu\text{m}$ . For the practical biomedical application of this approach three important developments are required. Firstly, the implementation of an image reconstruction method that is appropriate for anatomically realistic target dimensions and geometries. For example, the phased array methods used in conventional pulse-echo ultrasound imaging could be employed. Secondly, the development of a transparent sensor head for backward mode imaging and thirdly some means of detecting the sensor output in parallel perhaps using a CCD or photodiode array rather than mechanically scanning a single detector element.

#### ACKNOWLEDGEMENTS

P. Beard is supported by an EPSRC Advanced Fellowship.

## REFERENCES

- <sup>1</sup> Kruger RA, Miller KD, Reynolds HE, Kiser Jr WL, Reinecke DR, Kruger GA. Contrast enhancement of breast cancer in vivo using thermoacoustic CT at 434 MHz. *Radiology*; 216: 279-283, 2000
- <sup>2</sup> Andreev VG, Karabutov AA, Solomatina SV, Savateeva EV, Aleynikov V, Zhulina YV, Fleming RD, Oraevsky AA, Optoacoustic tomography of breast cancer with arc-array-transducer, *Proc SPIE Vol 3916*, pp36-47, 2000
- <sup>3</sup> Hoelen CG, de Mul FFM, Pongers R, Dekker A, , Three-dimensional photoacoustic imaging of blood vessels in tissue, *Optics Letters*, Vol 23, No 8, pp648-650, 1998
- <sup>4</sup> Paltauf G and Schmidt-Kloiber H, Optical method for two dimensional ultrasonic detection, *Applied Physics Letters*, Vol 75, No 8, pp1048-1050, 1999
- <sup>5</sup> Kallman, Jeffrey S.; Ashby, A. E.; Ciarlo, Dino R.; Thomas, Graham H.; OPUS: an optically parallel ultrasound sensor, *Proc. SPIE Vol. 3912*, p. 64-73, 2000
- <sup>6</sup> Hamilton JD and O'Donnell M, High frequency ultrasound imaging with optical arrays, *IEEE Transactions on Ultrasonics, Ferroelectrics and Frequency Control*, Vol 45, No 1, pp216-235, 1998
- <sup>7</sup> Wilkens V. and Koch Ch., Optical multilayer detection array for fast ultrasonic field mapping, *Optics Letters*, Vol 24, No 15, pp1026-1028, 1999
- <sup>8</sup> JD Hamilton, T. Buma, M. Spisar, and M. O'Donnell, High Frequency Optoacoustic Arrays Using Etalon Detection, *IEEE Transactions on Ultrasonics, Ferroelectrics and Frequency control*, Vol 47, No1, p160-169, 2000
- <sup>9</sup> Beard PC, Perennes F, Draguioti E, Mills TN, An optical fibre photoacoustic-photothermal probe, *Optics Letters*, Volume 23, Issue 15, pp. 1235-1237, 1998
- <sup>10</sup> Beard PC, Hurrell A, Mills TN, Characterisation of a polymer film optical fibre hydrophone for the measurement of ultrasound fields for use in the range 1-20MHz: a comparison with PVDF needle and membrane hydrophones, *IEEE Transactions on Ultrasonics, Ferroelectrics and Frequency control*, Vol 47, No1, p256-264, 2000
- <sup>11</sup> Beard PC, Perennes F, Mills TN, Transduction mechanisms of the Fabry Perot polymer film sensing concept for wideband ultrasound detection., *IEEE Transactions on Ultrasonics, Ferroelectrics and Frequency control*, Vol 46, No 6, pp1575-1582, 1999
- <sup>12</sup> Uno Y and Nakamura K, Pressure sensitivity of a fibre-optic microprobe for high frequency ultrasonic field, *Jpn. J. Appl.Phys.*, Vol 38, pp3120-3123, 1999
- <sup>13</sup> Beard PC and Mills TN, A 2D optical ultrasound array using a polymer film sensing interferometer, *IEEE Ultrasonics Symposium 2000*, in press.
- <sup>14</sup> Beard PC and Mills TN, An optical detection system for biomedical photoacoustic imaging, *Proc. SPIE 3916*, pp100-109, 2000
- <sup>15</sup> Troy TA, Page DL, Sevic-Mucraca EM, Optical properties of normal and diseased breast tissues: prognosis for optical mammography, *J Biomed Optics*, 1(3), pp342-355, 1996
- <sup>16</sup> Simpson, C.R., Kohl, M., Essenpreis, M., Cope, M., "Near-infrared optical properties of ex vivo human skin and subcutaneous tissues measured using the Monte Carlo inversion technique," *Phys. Med. Biol.* 43, 2465-2478 (1998).
- <sup>17</sup> Roggan A, Friebel M, Dorschel K, Hahn A, Muller G, Optical properties of circulating human blood in the wavelength range 400-2500nm, *Journal of Biomedical Optics*, 4(1), pp36-46, 1999
- <sup>18</sup> British Standard, BS EN60825-1, 1994
- <sup>19</sup> Steinberg BD, Principles of aperture and array design, John Wiley Inc, 1976
- <sup>20</sup> Paltauf, Guenther; Schmidt-Kloiber, Heinz; Koestli, Kornel P.; Frenz, Martin; Weber, Heinz P., Optoacoustic imaging using two-dimensional ultrasonic detection, *Proc. SPIE Vol. 3916*, p. 240-248, 2000